

## Turbine Blading Performance Evaluation Using Geometry Scanning and Flowfield Prediction Tools

Pavlos K. Zachos<sup>1</sup> Maria Pappa<sup>2</sup> Anestis I. Kalfas<sup>2</sup> Gabriel Mansour<sup>2</sup> Ioannis Tsiafis<sup>2</sup> Pericles Pilidis<sup>1</sup>  
Hiroharu Ohyama<sup>3</sup> Eiichiro Watanabe<sup>3</sup>

<sup>1</sup>Department of Power & Propulsion, School of Engineering, Cranfield University, MK43 0AP, Cranfield, UK  
E-mail: p.zachos@cranfield.ac.uk

<sup>2</sup>Department of Mechanical Engineering, Aristotle University of Thessaloniki, 54124, Thessaloniki, Greece

<sup>3</sup>Turbine Engineering Department, Mitsubishi Heavy Industries, Takasago Machinery Works, Takasago Hyogo 676, Japan

*Keywords: Turbines, Geometry Scanning, Camber Line Deformation, Performance Prediction*

### Abstract

This paper investigates the effect of blade deformation, caused by manufacturing inaccuracies, on the performance of a 2-stage axial steam turbine. A high fidelity 3D coordinate Measurement Machine has been employed to obtain the exact geometrical model of the blades. A Streamline Curvature solver was used to predict the overall performance of the turbine.

During the manufacturing process of the casts and of the blades themselves, several types of errors can occur which lead to a different geometry from that envisaged by the designer. The main objective of this study is to investigate the effect of those errors on the performance of a 2-stage experimental axial steam turbine. A high fidelity measurement of the actual geometry of both stator and rotor blades has been carried out, using a 3D Coordinate Measurement Machine. The cross sections of the blades obtained by the measurement were compared with those produced by the design process to evaluate the change in blade inlet/exit angles. In addition, the geometrical deviations from the initial design have been subjected to a statistical study in order to locate the nature of the error. The actual (measured) model has been used as input into a Streamline Curvature solver to evaluate its performance. Finally, a comparison with the performance plots of the original geometry has been carried out.

A measurable change of efficiency as well as in the total power delivered by the turbine was found. This suggests that the accumulated error caused during the manufacturing procedure plays a significant role in the overall performance of the machine by making it less efficient by more than 1%. Reverse engineering techniques are proposed to predict and alleviate these errors leading thereby to a final design of each stage with improved performance.

### Nomenclature

CAD Computer Aided Design

CMM	Coordinate Measurement Machine
N	Number of measurement points
PS	Pressure Side
QO	Quasi-orthogonal location
R	Rotor
S	Stator
SLEQ	Streamline Equilibrium solver
SS	Suction Side
v	Cylindrical coordinate on blade
x	Axial direction
x <sub>1</sub>	Blade's inlet angle
x <sub>2</sub>	Blade's exit angle
y	Vertical direction
Greek	
α	Pearson index defining skewness
α <sub>4</sub>	Pearson index defining kurtosis
θ	Camber angle
μ <sub>v</sub>	v-order statistical moment

### Introduction

A 3D Coordinate Measurement Machine facility (CMM) of the latest technology enables both researchers and industrial manufacturers to evaluate the precision of several different manufacturing techniques that have been applied for the production of a mechanical component. This is, undoubtedly, a time efficient technique offering a good level of accuracy<sup>1</sup>. Especially when the examined component is a turbine blade, larger errors can occur during the manufacturing procedure. These errors have a stronger impact to the final performance. Regarding their origin, geometry inaccuracies can be accumulated during the manufacturing procedure of the mould as well as during the investment casting of the blade itself. They can be compiled as deformations of the blade camber line or surface degradations<sup>2</sup>. Heat transfer effects during the cooling of the cast blade also play a major role in geometry deformations, which combined with the former can lead to a quite significant change in performance as well as in the mechanical integrity of the component<sup>3,4</sup>. Usually, the state-of-the-art blades used in real engines are subject to very tight dimensional and surface tolerances posed by the manufacturer and there is little chance for an incorrectly manufactured part to be used.

However, is highly possible for a bad quality component to be produced and put on the field, when it is designated for preliminary blade performance assessments or experimental cases, where the quality control of the geometry is poor or sometimes absent and the manufacturing techniques of relatively limited precision.

Consequently, the evaluation of aerothermodynamic and mechanical properties of the actual blade compared to the design intent, are of great importance. The designer can apply reverse engineering techniques to eliminate systematic manufacturing errors<sup>5-6)</sup>. The researcher is provided with an improved understanding of the on-the-field engine.

This paper examines the camber line deformation effect on the performance of the 2-stage experimental axial steam turbine<sup>7-8)</sup> based on a high fidelity CMM inspection of the actual geometry. A statistical study of the geometrical errors aims to unveil the nature and the significance of the aforesaid inaccuracies.

### Error Evaluation and Numerical Approach

#### Geometry Scanning

The 2-stage high pressure steam turbine used in the present work is described in great detail by Chaluvadi et al<sup>7-8)</sup>. Its aerothermodynamic properties as well as some geometrical features are summarized in Table 1.

For the 3D representation of both stator (Nozzle Guide Vanes) and rotor blades (Fig.3a), a resolution of 1 point / 2 mm<sup>2</sup> for each blade has been chosen. These points are measured by a Coordinate Measuring Machine (CMM) which is illustrated in the following figure.

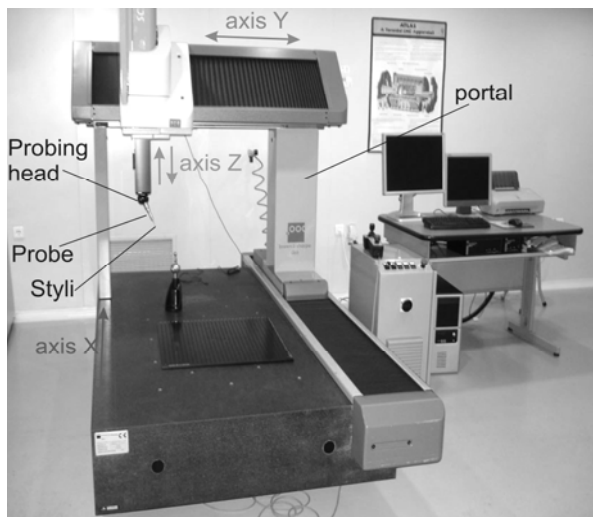


Fig. 1 Coordinate Measurement Machine (CMM)

For the CMM measurement a PH10MQ probing head has been used, which is able to inspect features at different angles without the need for frequent, time-consuming, styli cluster changes. A repeatability of 0.5µm at 62mm radius can be achieved with the

PH10MQ probe head, providing accurate positioning even when using long extensions.

In addition, a TP200 probe has been employed, with a styli extension of 10mm. The TP200 probe uses micro strain gauge transducers to deliver excellent repeatability and accurate 3D form measurement even with longer stylus. The trigger force (at styli tip) is 0.02N for XY plane and 0.07N for Z plane.

The styli used for this measurement was a straight styli. It incorporates highly spherical industrial ruby ball. It is of low density keeping tip mass to a minimum, which avoids unwanted probe triggers caused by machine motion or vibration. The styli used in this work was TIP 2mm by 10mm (A=2mm, D=10mm) and its geometry is represented in the following figure.

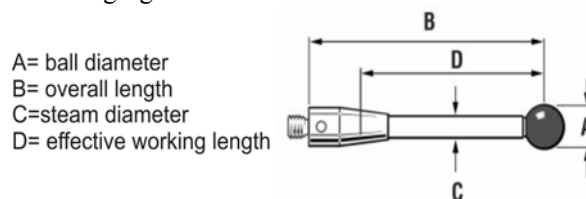


Fig. 2 Styli terminology

The measurements have been conducted in respect to a fixed reference system.

The output of each measurement is a point cloud for each blade, which in fact represents the 3D geometry of the blades (Fig.3b).

In order to compare the 3D model with the theoretical design of each blade (CAD sections), a 2D cross section generation in certain radial positions advised by the theoretical data is required. Using specific design programs a set of ten (10) cross sections for each blade has been obtained (Fig.3c).

Splines have been used for generation of more points, in every case that the measured points are not enough for the comparison. The error introduced by this transformation has been proved to be <0.5%<sup>5)</sup> depending on the total number of points in the cloud.

The 2D cross sections of the measurement are compared to the theoretical design of the blade in the following sections. The evaluation of the geometry errors is also presented.

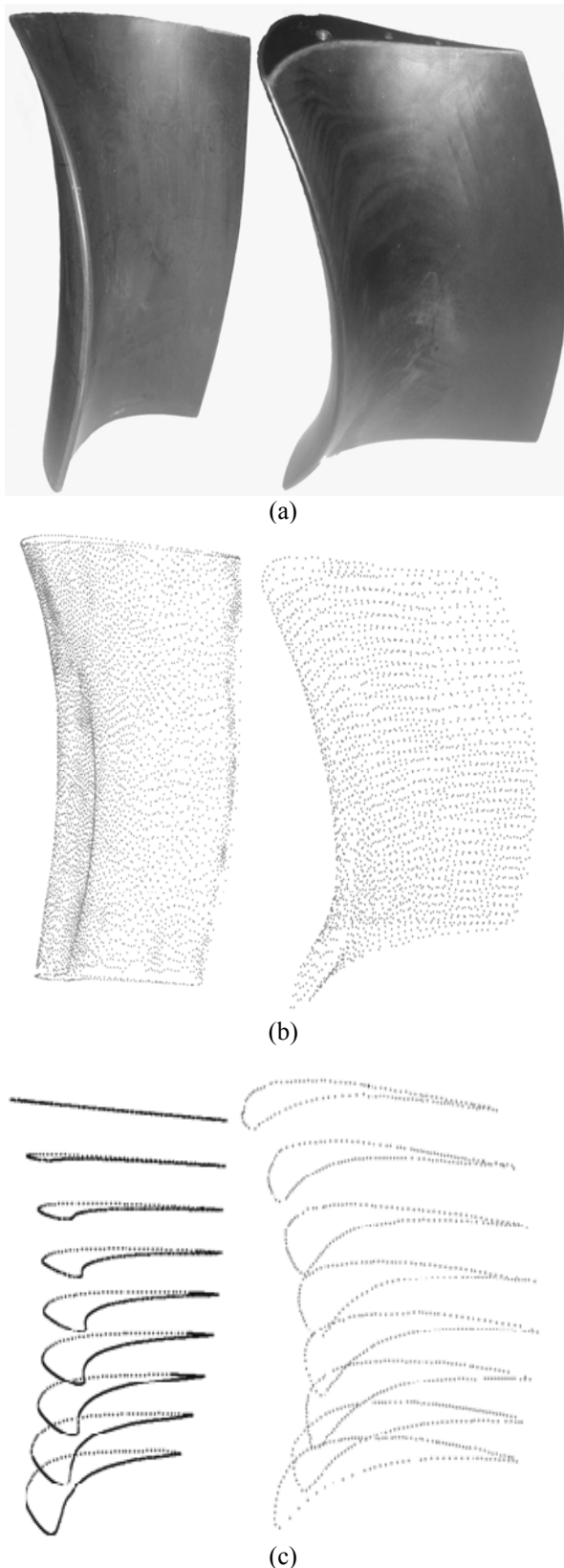


Fig. 3 (a) Rotor (left) and stator (right) blade models  
 (b) Point cloud measurements (c) Cross Sections

### Comparison with the Design Intent

As soon as the 2D cross sections of the rotor and stator blade have been generated, a section-to-section matching with the theoretical design is carried out. The output of this analysis is the deviation of the measured (CMM) geometry from the theoretical design (CAD) by means of normal distance from the latter. The assumptions-requirements done in order the comparison to be valid are (i) both blades (measurement and CAD) are compared in zero stagger angle, which means their cord should be parallel to the horizontal axis and (ii) both blades have the same leading edge. For those reasons, some moves and rotations of the clustered cross section points in the two dimensional space is applied. The output of the matching algorithm is presented in fig.4 for a section of the rotor blade. The deviation between the two lines which leads to a different inlet as well as exit blade angle is distinguishable. The correct calculation of the angle change is a matter of accuracy since the order of magnitude of this change takes values in a range between 2°-3°. Further discussion about this issue will be held in the next sections. Similar plots are generated for every 2D section of rotor and stator blades. It is reminded that the camber lines are calculated using the formula:

$$x = \frac{x_{SS} + x_{PS}}{2} \quad (1)$$

$$y = \frac{y_{SS} + y_{PS}}{2} \quad (2)$$

For the analysis of the surface errors, the definition of a parameter  $v$  on the 2D cross section of each blade is required (Fig.4 top). Parameter  $v$  is a non-dimensional arc-length parameter (percentage of arc length of blade contour). The surface error in direction  $v$  is defined as the normal distance between the CAD and the measured geometry in each side of the 2D cross section profile. Therefore, an error plot (Fig.4 bottom) can be introduced for each one of the ten cross sections of each blade, in which the deviation between the two geometries is illustrated.

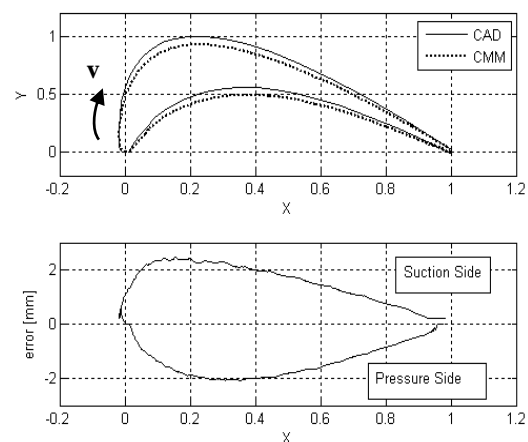


Fig. 4 Profile matching (top) and geometry deviation (bottom) between CAD and measured cross section for the rotor blade

A statistical assessment of the error distribution has been also carried out in order its nature to be investigated.

For every cross section the mean value and the first four (4) statistical moments have been calculated. It is reminded that the v-order moment in terms of the mean value of the variable is defined as:

$$\mu_v = \frac{1}{N} \sum_{i=1}^N (x_i - \bar{x})^v \quad (3)$$

Pearson has used the first four moments in order to define the skewness and the kurtosis of a distribution. Particularly, the index

$$\alpha^2 = \frac{\mu_3^2}{\mu_2^3} + 4 \quad (4)$$

characterizes the distribution as symmetric if  $\alpha=2$  or non-symmetric (positive- or negative- skewed) if  $\alpha>2$ . In addition, the index

$$\alpha_4 = \frac{\mu_4}{\mu_2^2} \quad (5)$$

takes a value equal to 3 for the normal distribution (mesokurtic), whereas  $\alpha_4>3$  for leptokurtic and  $\alpha_4<3$  for platykurtic distribution.

Regarding the error distribution properties, the values of the above parameters are illustrated in the following figures (Fig.7 and 8) for the suction and pressure side errors of the rotor and stator blade correspondingly. The distribution of the mean value of the errors for each cross section is presented in figures 5 and 6.

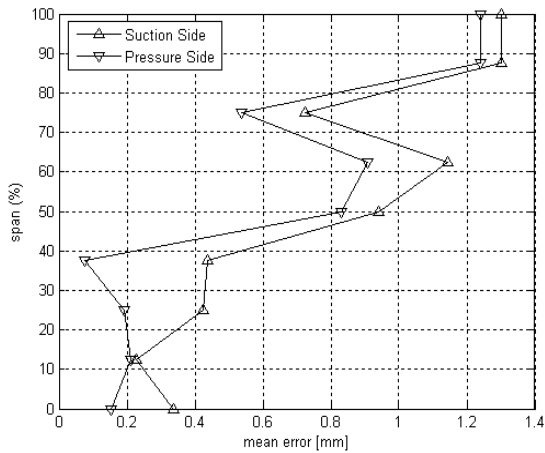


Fig. 5 Error mean values for the rotor blade cross sections

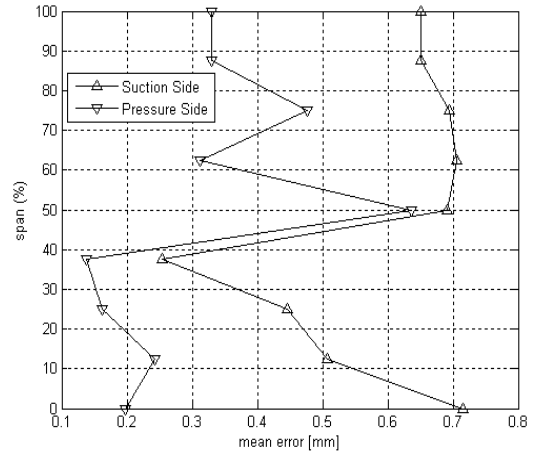


Fig. 6 Error mean values for the stator blade cross sections

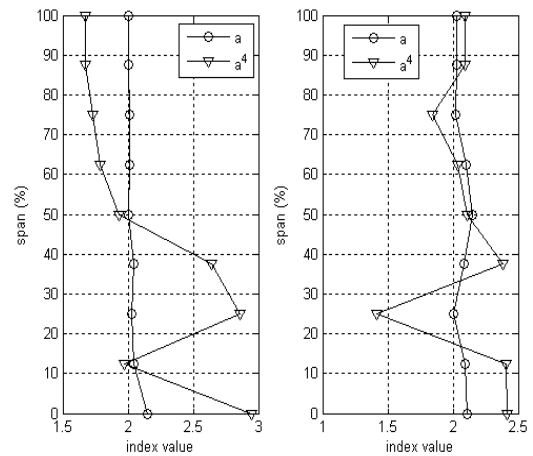


Fig. 7 Pearson index values for the suction side (left) and the pressure side (right) of the rotor blade

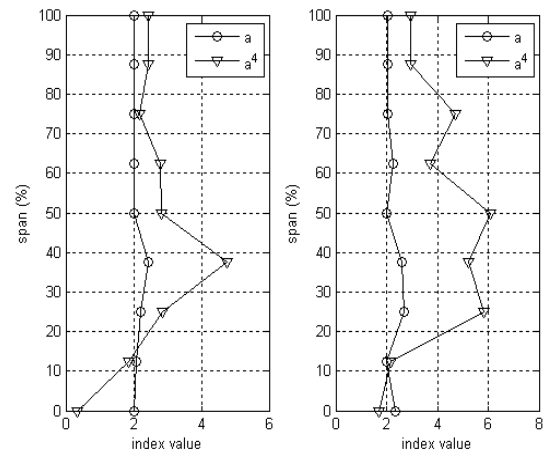


Fig. 8 Pearson index values for the suction side (left) and the pressure side (right) of the stator blade

Useful remarks and conclusions regarding the nature of the geometrical error can be made from the plots above. A more extensive discussion is included in the following sections.

### Camber Line Deformation

The deviation between the theoretical and the measured geometry presented in the previous sections can be compiled into a camber line deformation of both blades. This aspect affects the aerothermodynamic properties of the turbine and should be investigated, since a camber line deformation introduces an alteration in both inlet and exit angle of the blade which is directly related with the stage velocity triangles formation.

The inlet/exit angles of a cross section are defined as illustrated in Fig.9 (schematic). Mainly, it is the angle between the x-axis and the tangent of the camber line in leading and trailing edge. The difference  $x_1-x_2$  is mostly known as camber angle  $\theta$ .

The values of the inlet and exit angle presented in Fig. 10 and 11 are valid for zero-staggered blade. Those values have nothing to do with the values when the stage is assembled and operating. However, this assumption does not affect the entire problem since it is the difference between the CAD and CMM values of actual interest and not the values themselves.

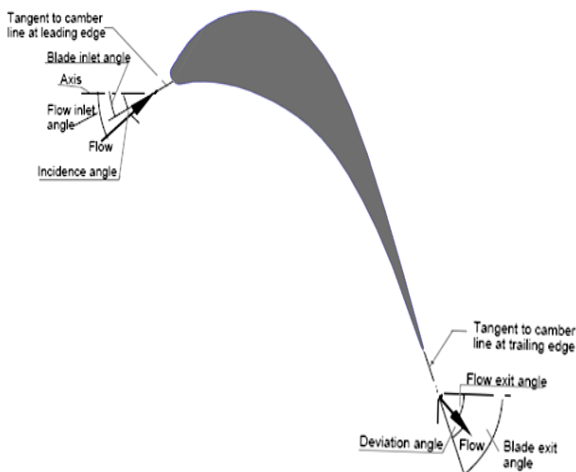


Fig. 9 Definition of blade's geometry

The mean camber line has been calculated for every cross section of the CAD as well as of the measured blades, based mainly on the formulas presented earlier. This procedure proved to be harder to be applied on the measured blades due to the unsmooth distribution of the CMM points. Therefore, a more sophisticated geometrical algorithm has been developed and applied for the allocation of the mean line of each cross section.

Since the camber line generation is finished,  $x_1$  and  $x_2$  angles can be easily calculated. Actually, as mentioned earlier, it is not the value of each angle which is of bigger interest, but the difference between the CAD and the measurement values for each cross section, in other words  $\Delta x_1$  and  $\Delta x_2$ .

The following figures (Fig.10 and 11) describe the inlet and exit angle distributions for the rotor and stator blade correspondingly.

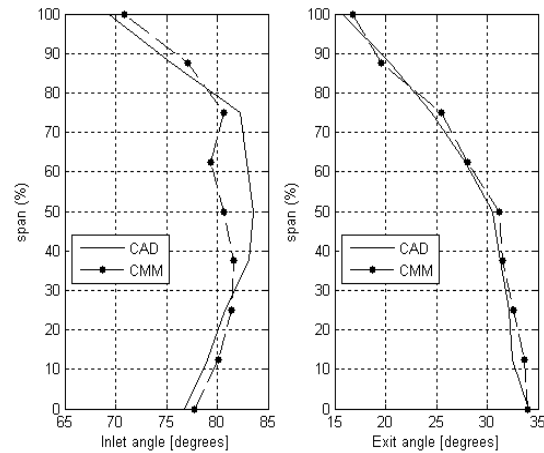


Fig. 10 Inlet and exit angle distribution for the rotor blade

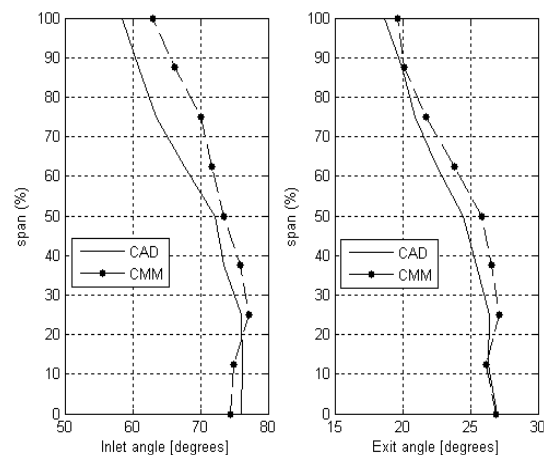


Fig. 11 Inlet and exit angle distribution for the stator blade

From the above figures can be assumed that the leading edge deformation of the camber line is stronger than the one on the trailing edge. Its effect on the performance of the stage will be investigated in the next sections with a streamline curvature zooming method. The only step required before that, is the transformation of the new geometry into an input file compatible with the streamline curvature code.

### Performance Evaluation of the Measured Geometry

In this section the effect of the geometry deformations in the total performance of the steam turbine is evaluated. Performance data of exactly the same test case based on experimental work as well as on steady and unsteady CFD simulations have been presented by Chaluvadi et al.<sup>7)</sup> In this work, a comparison of the stage performance based on Denton's streamline curvature code SLEQ will be presented. This code has been developed as a tool for predicting the flow in steam turbines. According to the author, it can also be used for gas turbines when choking prevents the use of other methods. There are three nested iterations into this code; the inner loop solves the continuity equation whereas the second

loop is the radial equilibrium iteration. Finally, the outer iteration loop updates the streamline curvature terms of the radial equilibrium equation and the slopes of the streamlines. A more detailed description of the algorithm is included in reference 10.

The turbine geometry and test conditions are described by Chaluvadi et al. <sup>7)</sup> and are also presented in the following table.

Table 1 Turbine geometry and test conditions (from reference 7)

	Stator	Rotor
Flow Coefficient ( $V_{x1}/U_m$ )		0.35
Stage Loading ( $\Delta h_0/U_m^2$ )		1.20
Stage Reaction		0.5
Mid-Span upstream Axial Gap (mm)		41.2
Hub-to-Tip Radius Ratio	0.8	0.8
Number of Blades	36	42
Mean Radius (m)	0.6858	0.6858
Rotational Speed (rpm)		550
Mid-span Chord	142.5	114.5
Mid-span Pitch-chord ratio	0.84	0.896
Aspect Ratio	1.07	1.33
Radial Shroud Clearance (mm)		1.0
Inlet Axial Velocity (m/sec)	13.85	
Mid-span Inlet Angle (from axial)	0°	13.46°
Mid-span Exit Angle (from axial)	71.03°	-70.86°
Chord Based Reynolds no.	$5.24 \times 10^5$	$4.12 \times 10^5$

Two separate runs of the code have been carried out, one for the CAD geometry and one for the measured. Regarding the geometry data, the code requires the blade inlet angle value in three (3) radial positions, whereas the exit angle of each blade is required in five (5) radial positions.

The input values as well as the deviation from the initial angles are presented in the following figures for the rotor and the stator blade correspondingly.

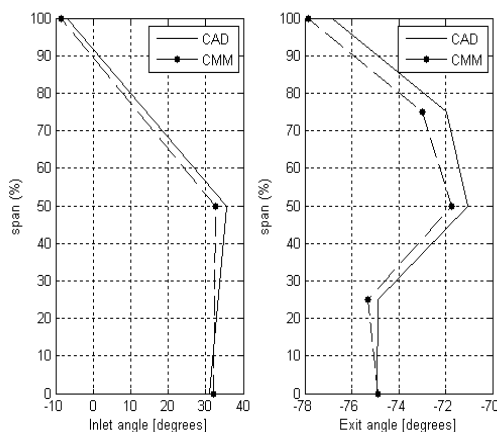


Fig. 12 Inlet and exit angle distribution in SLEQ's input file for the rotor blade

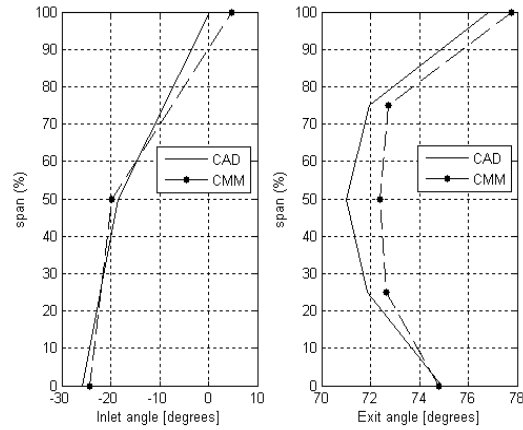


Fig. 13 Inlet and exit angle distribution in SLEQ's input file for the stator blade

The axial locations within the stages where flow data are available are presented in fig.14. There also three locations upstream of position 4 (LE of stator 1) and three more downstream of position 11 (TE of rotor 2). Uniform flow boundary conditions are applied on locations 1 and 14.

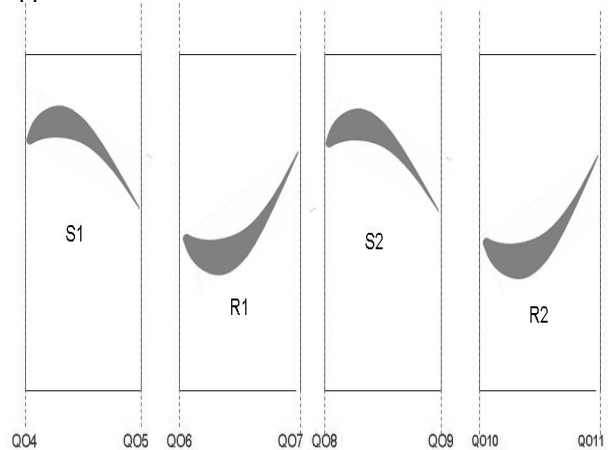


Fig. 14 Stage locations

## Results and Discussion

### Streamline Curvature Results

In this section the output results from the streamline equilibrium code are presented. Locations 7 and 11 are of greater importance because they indicate the exit of each stage and therefore most of the result plots concern those points. Some results regarding the overall performance of the 2-stage configuration can be calculated as well. For every property a second plot illustrating the change of the value in terms of the span is presented. The deviation from the datum (CAD) value is defined as:

$$\Delta V = \frac{Value(CMM) - Value(CAD)}{|Value(CAD)|} \quad (6)$$

This way the increase/decrease of the initial (CAD) value can be better indicated.

The Streamline Curvature simulation offers the great advantage of evaluating several different properties without any further post-processing of the results. Many plots, depicting the effect of the blade line deformation in the overall performance of the 2-stage turbine have come out from the code. However, only the efficiency comparison for every stage is presented in the following plots because it is considered to be the most representative property which indicates the effect of the errors in the geometry.

The simulation is, as mentioned earlier, an iterative procedure until the convergence of the system. It can be observed that for the specific testcase there are non-zero incidence angles into the blades. That implies that the turbine is not working at its design point but at an off-design point defined by the specified in the input file mass flow and rpm.

The efficiency plots of each stage are presented in the following figures.

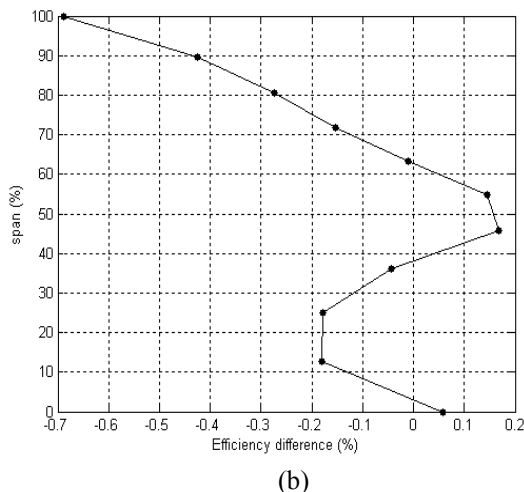
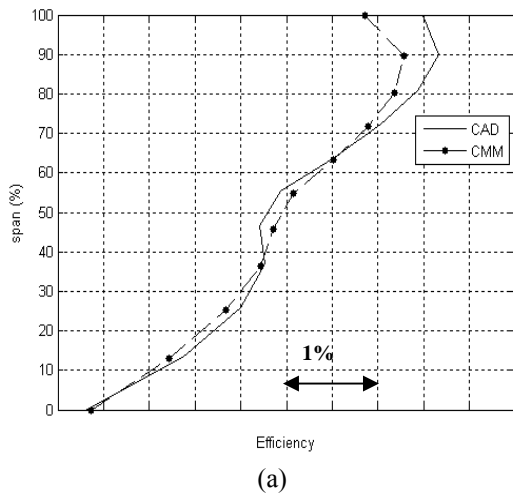


Fig. 15 (a) First stage cross section efficiency distribution and (b) efficiency deviation

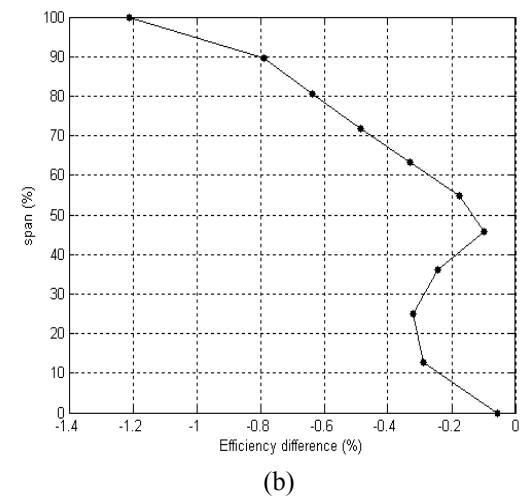
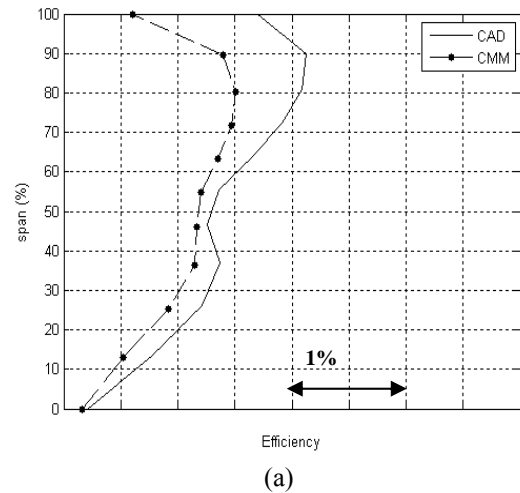


Fig. 16 (a) Second stage cross section efficiency distribution and (b) efficiency deviation

As shown above, the efficiency deviation between the two cases is significant, which is expected because of the geometry errors illustrated earlier. An increase in the pressure loss of each stage has been also observed from the SLEQ results.

A 4.66% decrease in the total output power of the turbine was observed as long as the CMM geometry is used as input to the SLEQ code for the performance simulation.

### Conclusions

In the current work a high fidelity 3D coordinate measurement device along with a streamline curvature academic solver have been used to determine the impact of the blade deformation on the performance of a 2-stage experimental steam turbine. The measurement has shown that the errors in the geometry, regardless of their origin, have led to a degradation of turbine's performance. The main conclusions from this study can be summarized as follows:

- The geometry scan measurement has indicated a measurable error of the order of  $\pm 0.5$  mm deviation from designed blade profile. This is

applicable both to rotor and stator blade. When the error is compiled in terms of blade's camber line deformation is more significant in the Leading Edge both for the rotor as well as for the stator blade. The deviation from the inlet angle design value is between 3-5%, whereas exit angle deviates no more than 1.5-2% from the design intent. In addition, this error is slightly increasing in the radial direction.

- A first statistical assessment of the error using the Pearson indices has shown that it follows a symmetric distribution but no conclusion can be made whether the distribution is normal or not since  $a_4$  has no constant value. Therefore, further research may be required regarding the origin of the error. However, in order this investigation to be valid a real and not an experimental turbine is required, mainly due to different technology used by the manufacturers for production line components.
- The Streamline Curvature solver has shown that the error in the geometry as expressed above has a non negligible impact in turbine's performance. The mass averaged efficiency has been decreased by approximately 1% for both blades which is significant for this kind of engines since they are designed to operate in the area of their maximum efficiency. Finally, the result of the deformation is a total output power decrease of the order of 5% compared to its design intent.

The present work illustrates the initial steps of a methodology developed to describe the impact of any kind of manufacturing errors on the performance of a gas or steam turbine. Further research on the nature of the geometry errors is required in order to distinguish and evaluate the impact of any random or systematic errors that may exist. Furthermore, a zooming method of higher fidelity (e.g. a CFD simulation of the flow field) than the streamline curvature approach could be employed in order to evaluate the exact nature of the inefficiencies of the deformed geometry. This approach is valuable since it provides the researcher with physical information (exact flow field) rather than only with their impact on the performance.

### Acknowledgements

The authors would like to acknowledge Professor John Denton and Professor Howard Hodson of Cambridge University Engineering Department for their valuable contribution, their insightful advice and their continuing support. Thanks are also due to Professor Denton for his kind permission to use his computational tools.

### References

- 1) Emmett, C., Phelan, P.: Quick check error verification of coordinate measuring machines, *Journal of Materials Processing Technology*, **155-156**, 2004, pp. 1207-1213.
- 2) Bons, J.: Turbine Surface Degradation with Service and its Effects on Performance, Brigham Young University, Technical report.
- 3) Prevey, P., Hornbach, D., Mason, P.: Thermal Residual Stress Relaxation and Distortion In Surface Enhanced Gas Turbine Engine Components, Proceedings of the 17<sup>th</sup> Heat Treating Society Conference and Exposition and the 1<sup>st</sup> International Heat Treating Symposium, Eds. D. L. Milam et al., ASM, Materials Park, OH, 1998, pp. 3-12.
- 4) Bae, J.S., Kyong, N.H., Seigler, T.M., Inman, D.J.: Aeroelastic Considerations on Shape Control of an Adaptive Wing, *Journal of Intelligent Material Systems and Structures* **16**, 2005, pp. 1051.
- 5) Mansour, G., Bouzakis, K.-D., Sagris, D., Varitis, E., Pappa, M.: Reverse engineering of parts using 3D measuring device (CMM) by means of splines, *ACTA TECHNICA NAPOCENCIS, Applied Mathematics and Mechanics*, **3**, 2006.
- 6) Yu-Shen, L., Jean-Claude, P., Jun-Hai, Y., Pi-Qiang, Y., Hui, Z., Jia-Guang, S., Karthik, R.: Automatic Least-Squares Projection of Points Onto Point Clouds with Applications in Reverse Engineering, *Elsevier, Computer-Aided Design*, **38** (12), 2006, pp. 1251-1263.
- 7) Chaluvadi, V.S.P., Kalfas, A.I., Hodson, H.P., Ohyama, H., Watanabe, E.: Blade row interaction in a high pressure steam turbine, *ASME Journal of Turbomachinery*, **125**, 2003, pp. 014-015.
- 8) Chaluvadi, V.S.P., Kalfas, A.I., Hodson, H.P.: Vortex transport and blade interactions in high pressure turbines, *ASME Journal of Turbomachinery*, **126**, 2004, pp. 395-405.
- 9) Hodson, H.P.: Blade Row Interactions in Low Pressure Turbines, *Von Karman Institute for Fluid Dynamics*, Lecture series 1998-02, 1998.
- 10) Denton, J.D.: Throughflow Program SLEQ, Computer User's Guide.
- 11) *The Jet Engine*, Rolls-Royce, 5th edition, 2005.
- 12) Saravanamuttoo, H.I.H., Rogers, G.F.C., Cohen, H.: *Gas Turbine Theory*, Prentice Hall, 5th edition, 2001.
- 13) Wilson, D.G.: The Design of High-Efficiency Turbomachinery and Gas Turbines, MIT Press, Cambridge, Massachusetts, 1984, Technical report.
- 14) Denton, J.D.: Through-flow Calculations for Transonic Axial Flow Turbines, *ASME Journal of Engineering for Power*, **100**, 1978, pp. 212-218.
- 15) Zwebek, A., Pilidis, P.: Degradation Effects on Combined Cycle Power Plant Performance – Part II: Steam Turbine Component Degradation Effects, *ASME Journal of Engineering for Gas Turbines and Power*, **125**, 2003, pp. 658-663.
- 16) Psinos, D.-P., *Statistics*, ed. Ziti, Thessaloniki, 1999.